Energy 182 (2019) 236–253

Contents lists available at ScienceDirect

Energy

journal homepage: www.elsevier.com/locate/energy

Practical heat pump and storage integration into non-continuous processes: A hybrid approach utilizing insight based and nonlinear programming techniques

Jan A. Stampfli [a, b, *], Martin J. Atkins [b], Donald G. Olsen [a], Michael R.W. Walmsley [b], Beat Wellig [a]

[a] Lucerne University of Applied Sciences and Arts, Competence Center Thermal Energy Systems and Process Engineering, Technikumstrasse 21, 6048, Horw, Switzerland
[b] University of Waikato, Energy Research Center, Private Bag 3105, Hamilton, 3240, New Zealand

ARTICLE INFO

Article history:
Received 18 January 2019
Received in revised form
21 May 2019
Accepted 30 May 2019
Available online 5 June 2019

Keywords:
Process integration
Pinch analysis
Mathematical programming
Multi-period
Industrial heat pump
Heat storage

ABSTRACT

This paper focuses on industrial heat pump (HP) integration in non-continuous processes. To achieve the necessary time-wise process decoupling of the HP system, heat recovery loops (HRLs) with stratified storages are used. This design type can be modeled as a mixed integer nonlinear programming problem which often results in expensive mathematical formulations. The challenge is addressed by a practical method that combines the insight based approach of Pinch Analysis with mathematical programming techniques to give the engineer more flexibility for the application of the method and to avoid long computation times. By the use of the insight based methods, the solution space of the mathematical formulation is restricted, and thus its complexity is reduced to a nonlinear programming problem optimizing the temperature levels in the HP-HRL system. As an objective, total annual costs (TAC) of the HP-HRL system are minimized. The developed hybrid method is applied to a dairy site and compared in terms of approach temperatures, temperature lift of the HP, TAC, and greenhouse gas emissions to the existing methods. It is shown, that the hybrid method provides realistic approach temperatures in contrast to the existing insight based method.

1. Introduction

In many industrial processes, energy efficiency and a reduction in greenhouse gas (GHG) emissions can be achieved by the integration of heat pumps (HPs). The key is the increased heat recovery (HR) that results by upgrading process waste heat with the HP to a higher temperature level in order to reduce process heating demand. Despite the advantages of HP integration, such as the reduction of operating costs, high investment costs are often a deterrent.

An additional deterrent is the high operational costs that can arise due to non-continuous process behavior [1]. In many industrial sites differences in the process schedules of individual plants or down time due to cleaning purposes make the integration of a HP a serious challenge. In particular, changes in the operating conditions for the compressor have a significant influence on its efficiency. This leads to higher operating costs, which further hampers the advantageous integration of HPs.

The next sections provide a brief review of existing methods for HP integration into continuous and non-continuous processes and details the research objectives aimed at alleviating the above noted deterrents. Owing to its importance and broad application in industry, the focus of this work lies on closed-cycle HPs equipped with mechanical compressors. The literature review is subdivided into insight based methods based on Pinch Analysis and mathematical programming methods.

1.1. Insight based methods

Several key papers from literature focusing on the proper integration of a HP based on pinch analysis have been published. The first approach for HP integration using insight based methods was

* Corresponding author. Lucerne University of Applied Sciences and Arts, Competence Center Thermal Energy Systems and Process Engineering, Technikumstrasse 21, 6048, Horw, Switzerland.
E-mail addresses: jan.stampfli@hslu.ch (J.A. Stampfli), martin.atkins@waikato.ac.nz (M.J. Atkins), donald.olsen@hslu.ch (D.G. Olsen), michael.walmsley@waikato.ac.nz (M.R.W. Walmsley), beat.wellig@hslu.ch (B. Wellig).

https://doi.org/10.1016/j.energy.2019.05.218

published by Townsend and Linnhoff [2]. Based on the Grand Composite Curve, the authors defined rules for HP integration in continuous processes. It was concluded, that only a HP which is integrated across the pinch temperature is thermodynamically beneficial. In order to address economic influences, Ranade [3] developed a formulation to determine a maximum temperature rise, which is identified as a tradeoff between compressor investment costs, operating costs and heat transfer investment costs of the heat exchanger network. A different approach developed by Wallin et al. [4] utilizes the Composite Curves to determine the optimal temperature level of the HP as well as the optimal HP size and type.

Insight based approaches as mentioned above are applied to several case studies such as a whiskey production process [5], a cheese factory [6], and a biomass gasification process by Pavlas et al. [7]. Olsen et al. [8] applied this graphic methodology to candy production to show how to handle discontinuities.

1.2. Mathematical programming methods

The first approach to HP integration through mathematical optimization was published by Shelton and Grossmann [9,10], using a mixed integer linear programming (MILP) formulation to highlight the economic potential of correctly integrated HP and cooling system networks. Based on the insight based approach from Townsend and Linnhoff [2], Colmenares and Seider [11] proposed a nonlinear programming (NLP) model for integration of cascaded HP cycles. Holiastos and Manousiouthakis [12] introduced an analytical approach for determining the optimal temperature levels of a reversible HP. The work was extended by a transportation formulation to determine a heat exchanger (HEX) and HP system [13]. Oluleye et al. [14] have developed a MILP approach for the integration of mechanical and absorption HP technologies as well as absorption heat transformers in combination with cogeneration systems for determining optimal temperature level, heat duties, as well as GHG emissions by minimizing total annual costs (TAC). Further, a framework for selecting the best HP technology using simplified HP models based on a correlation between real and ideal thermodynamic cycles was published by Oluleye et al. [15] and was extended to minimize exergy degradation [16]. A mixed integer nonlinear programming (MINLP) formulation is published by Wallerand et al. [17] whereby detailed HP models are developed considering effects such as sub-cooling, multi-stage phase changes, and refrigeration selection.

Maréchal and Favrat [18] developed a method for optimal energy conversion unit integration by including exergy factors. This work was continued by considering multiple utility pinches by Becker et al. [19]. A multi-objective MILP optimization on operating and investment cost for single, multi-stage and combination of multiple HPs is applied including refrigeration selection by Becker et al. [20]. Also, the model was extended to non-continuous processes [21] by using the Time Slice Model and a cascaded thermal energy storage (TES) system. This model was applied to a case study of a cheese factory [22].

Methodologies for HP integration considering non-continuous processes are applied for several case studies such as residual wastewater upgrading of a shower [23]. Further, Miah et al. [24] developed a methodology for HP integration in simple and complex factories and was applied to a large non-continuous confectionery factory with multiple production zones.

1.3. Research objectives

HP integration in non-continuous processes is usually tackled by sophisticated mathematical programming formulations. Thus such approaches are usually formulated as MINLP problems they tend to be expensive in terms of computing time and resources and limit the flexibility of the method by its application. In practical applications, the optimization step should be as short as possible to prevent long interruptions in the workflow. In order to address the challenge of a practical HP integration in non-continuous processes the following objectives have to be fulfilled:

(1) Practicality: having a high degree of flexibility by the application of the method
(2) Optimality: finding an optimal solutions
(3) Applicability: having a short computation time

Objective (1) is usually achieved using insight based methods. Therefore, in a previous work, an insight based approach [25] using heat recovery loops (HRLs) [26] for time-wise decoupling of the process was developed. The introduced COP Curves, the Time Slice Model [27] and the Supply & Demand Curves [28] serve as graphic design tools for HP and TES design. However, the resulting HP-HRL system tends to have large approach temperatures in the condenser and evaporator which is not realistic and thus does not fulfill objective (2). This can be attributed to the fact that the insight based method does not consider all economic aspects in the optimization process. Therefore, further work was performed using a nonlinear programming (NLP) formulation for the optimization of the condensation, evaporation and the storage temperatures levels by minimization of TAC [29].

Objective (3) can only be addressed by avoiding the use of expensive mathematical programming methods. Therefore, in this paper, a hybrid method is developed by unifying the existing insight based [25] and mathematical programming [29] approaches. By utilization of insight based method for decision making, the original MINLP problem can be reduced to NLP problem which reduces computation time sharply. The NLP formulation is also extended with rebalancing utility within the HP-HRL system to cover changes in condenser and evaporator heat flow caused by changing coefficient of performance of the HP. To demonstrate the applicability of the hybrid method, the production of raw materials for butter production in a large dairy site is analyzed as a case study using a Total Site Heat Integration approach.

2. Methods

In this section, a practical method for industrial heat pump (HP) integration into non-continuous processes is introduced. The method consists of seven steps and an overview is shown in Fig. 1. In particular, steps 3 to 5 are based on pinch techniques and step 6 involves the nonlinear programming (NLP) formulation.

2.1. Step 1 – extraction of process data

First, the process requirements have to be identified. Therefore, process stream data has to be analyzed to identify heating and cooling requirements. By investigating non-continuous processes, the scheduling of the process is crucial for the identification of the energy targets. In addition, for an economic evaluation investment costs for equipment, operating costs as well as economic coefficients such as the interest rate and investment period have to be identified.

2.2. Step 2 – identification of energy targets

By the use of the Time Slice Model non-continuous processes are broken down into time slices (TSs). Each of these TSs represents

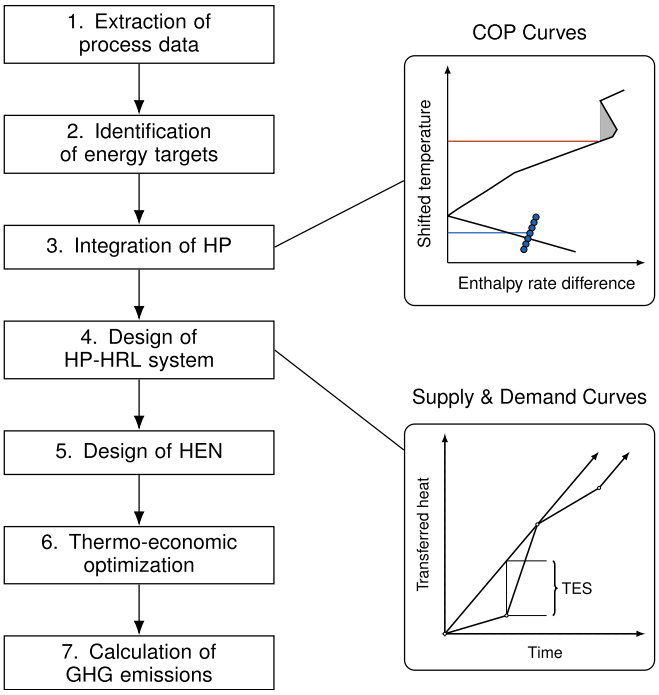

Fig. 1. Procedure for HP integration into non-continuous processes.

a time duration in which the process has a continuous behavior. A change in heating or cooling requirements indicates the end of the actual TS and the start of the next TS. For the identification of the energy targets the heat cascade for each TS is applied. By selecting an overall ΔT_{min}, a specific Grand Composite Curve (GCC), as well as the pinch temperature is obtained for each TS.

2.3. Step 3 – integration of heat pump

Typically, the change in process requirement, as identified in step 2, would lead to varying operation conditions for the HP resulting in lower compressor efficiency. In order to overcome this challenge, constant condensation and evaporation temperatures are searched at which the HP can run throughout the entire process duration.

For the integration of the HP, the GCC is used. Thereby, the rule integrating a HP across the pinch defined by Townsend and Linnhoff [2] is also valid for non-continuous processes. To cover variations in process requirements, on both sides of the HP, heat recovery loops (HRLs) including stratified thermal energy storages (TESs) are used to transfer the heat from or to the process. As a result, additional heat exchangers (HEXs) are required since the HP evaporator and condenser are not directly connected to the process. This results in a higher temperature difference ΔT between process stream and condensation or evaporator temperature as given by

$$\Delta T = \Delta T_s + 2\Delta T_{HRL} + \Delta T_{HP} \tag{1}$$

represented as the sum of the contributed temperature differences ΔT_{cont} of all included streams. Thereby, different contributed temperature differences are defined for each stream of the process(es) (subscript s), the HRL, and the condensation, or the evaporation of the HP. Thereby, the shifted temperature of a stream is given by

$$T^* = T - \Delta T_{cont} \qquad \text{for hot streams and} \tag{2}$$

$$T^* = T + \Delta T_{cont} \qquad \text{for cold streams.} \tag{3}$$

Usually, the contributed temperature difference is given by $\Delta T_{cont} = \Delta T_{min}/2$. Thereby, ΔT_{min} represents the minimum temperature difference at the pinch. According to Kemp [30], temperature contributions can be adapted individually for each stream having an unusually high or low film heat transfer coefficient. In this work, the temperature contributions are applied as follows:

- Process streams: normal heat transfer coefficients are assumed, and therefore the standard temperature contributions of $\Delta T_s = \Delta T_{min}/2$ are applied.
- HRL: the media in the HRL is water and therefore also the standard temperature differences of $\Delta T_{HLR} = \Delta T_{min}/2$ are applied.
- Condensation and evaporation in HP: due to the high film heat transfer coefficients during the phase change of the refrigerant the temperature contributions are reduced to $\Delta T_{HP} = \Delta T_{min}/4$.

Therefore, the resulting temperature difference between process streams and HP as given in Eq. (1) is resulting in

$$\Delta T = \underbrace{\frac{1}{2}\Delta T_{min} + \frac{1}{2}\Delta T_{min}}_{\text{process from/to HRL}} + \underbrace{\frac{1}{2}\Delta T_{min} + \frac{1}{4}\Delta T_{min}}_{\text{HRL from/to HP}} = \frac{7}{4}\Delta T_{min}. \tag{4}$$

Thus, in the GCC condensation and evaporation temperatures of the HP are already shifted in respect to the process stream by $\pm\Delta T_{min}/2$, the relation between shifted and real temperatures is given as follows:

$$T_{co} = T^*_{co} + \frac{5}{4}\Delta T_{min} \tag{5}$$

$$T_{ev} = T^*_{ev} - \frac{5}{4}\Delta T_{min} \tag{6}$$

In order to identify optimal operating conditions for the HP, it is first investigated how the absorbed and emitted heat flows at constant condensation and evaporation temperatures match the heating and cooling requirements of the process in each TS. Therefore, a shifted overall condensation temperature $T^*_{co,sel}$ has to be selected, whereby the heat flow emitted by the HP is as high as possible (maximize heat recovery) and the condensation temperature as close as possible to the pinch temperature T_P (minimize the temperature lift of the HP). To prevent the increase of utility need, self-sufficient pockets must not be destroyed as shown in Fig. 2.

To find the optimal evaporation temperature $T_{ev,opt}$, the so-called COP Curves are used. These curves describe the absorbed heat flow of the HP $\dot{Q}_{a,l}$ as a function of the temperature levels of condensation T_{co} and evaporation T_{ev}. The formulation is based on the coefficient of performance (COP) and the energy balance of the HP. The HP cycle is formulated as a Carnot cycle using a 2nd law efficiency ζ for each TS (subscript l) as follows:

$$\mathrm{COP}_l = \zeta \frac{T_{co,sel}}{T_{co,sel} - T_{ev}} = \frac{\dot{Q}_{e,l}}{P_{el,l}} \tag{7}$$

To ensure practicality, the value of the 2nd law efficiency is set to a conservative value of 0.35. Considering an open type compressor, the energy balance for the HP is given by

$$\dot{Q}_{e,l} = \dot{Q}_{a,l} + P_{el,l}\,\eta_{drive} \tag{8}$$

where η_{drive} describes the drive efficiency of the compressor with a

value of 0.9 [31]. By the use of Eq. (7) and Eq. (8), for a selected condenser temperature $T^*_{co,sel}$ the resulting absorbed heat flow by the evaporator $\dot{Q}_{a,l}$ can be calculated as a function of T^*_{ev} between the lowest temperature of the GCC $T^*_{GCC,min} = T^*_{ev,min}$ and the pinch temperature $T_P = T^*_{ev,max}$. In Fig. 2, the resulting COP Curve is plotted as a blue dotted curve (each dot represents a computed point) for each TS.

At the intersection between the COP Curve and the GCC, the cooling requirements of the process and the absorbed heat flow by the HP coincide with each other. If the evaporator temperature is below the intersection, not enough heat flow can be absorbed by the HP to cover the cooling demand of the process, and TESs have to be included. Therefore, the heat surplus of the process $\Delta\dot{Q}^+_{TES,l}$ shown in Fig. 2 (a) has to be transferred to the TES. If the evaporator temperature is above the intersection, more heat flow is absorbed by the HP as provided by the process. Therefore, additional heat from the TES $\Delta\dot{Q}^-_{TES,l}$ has to be provided to the HP. By solving

$$\sum_{l=1}^{L} \Delta\dot{Q}^+_{TES,l}\left(T^*_{ev,opt}\right)\Delta t_l = \sum_{l=1}^{L} \Delta\dot{Q}^-_{TES,l}\left(T^*_{ev,opt}\right)\Delta t_l \quad (9)$$

where Δt_l represents the duration of a TS, the optimal shifted evaporation temperature level $T^*_{ev,opt}$ is found where heat surpluses and heat deficits of all TSs ($l = 1 \ldots L$) are equal. The resulting condensation temperature $T_{co,sel}$ and evaporator temperature $T_{ev,opt}$ are used in step 6 as initial conditions for the thermo-economic optimization.

2.4. Step 4 – design of heat pump and heat recovery loop system

In order to define the required HP and TES sizes, the Supply & Demand Curves developed as a part of the Time Pinch Analysis by Wang and Smith [28] are used. By the use of these curves, the optimal utility system can be designed by minimizing the supplied heat flow.

In contrast to the Time Slice Model, the Supply & Demand Curves consider time constraints first and then temperature constraints and thus no heat transfer backward in time is possible. In Fig. 3, the optimization procedure for designing the HP-HRL system using the Supply & Demand Curves in the $\Delta Q, t$-chart is shown. Thereby, transferred heat between the HP and the process streams over time is shown. The supply curve represents what is provided by the HP and the demand curve what needs to be provided by the HP-HRL system to the process. For the design of the HP-HRL system both sides of the HP has to be analyzed, and therefore this procedure has to be applied to the emitted heat by the condenser and the absorbed heat by the evaporator of the HP.

As an example in Fig. 3, the maximal demand from the process is 40 kW in the time interval 8–16 h. If there is no TES, the HP has to be designed for this heat flow as shown as, “Supply without TES”. As a result, the demand for transferred heat can be provided in 8 h, whereby the process runs for 24 h. This results in an oversized HP and thus in higher investment costs.

By increasing the operation duration of the HP for the same amount of transferred heat and introducing TESs, the supply heat flow can be reduced till a time pinch occurs as supply and demand curve touch. A further reduction in supply would lead to a lack of transferred energy to the process, and thus heat cannot be transferred backward in time resulting in an infeasible solution.

As shown in Fig. 3 the minimal possible supply for a 24 h operation duration of the HP is 17 kW, resulting in a starting time 6 h before the process (−6 h at x-axis). Therefore a TES with 198 kWh capacity has to be integrated which has to store the heat surplus in the time interval −6 to 8 h and release the heat in the time interval 8–16 h to cover the insufficient heat flow provided by the HP.

The resulting emitted heat flow, the absorbed heat flow, and the capacities of the TESs are used in step 6 as input values for the

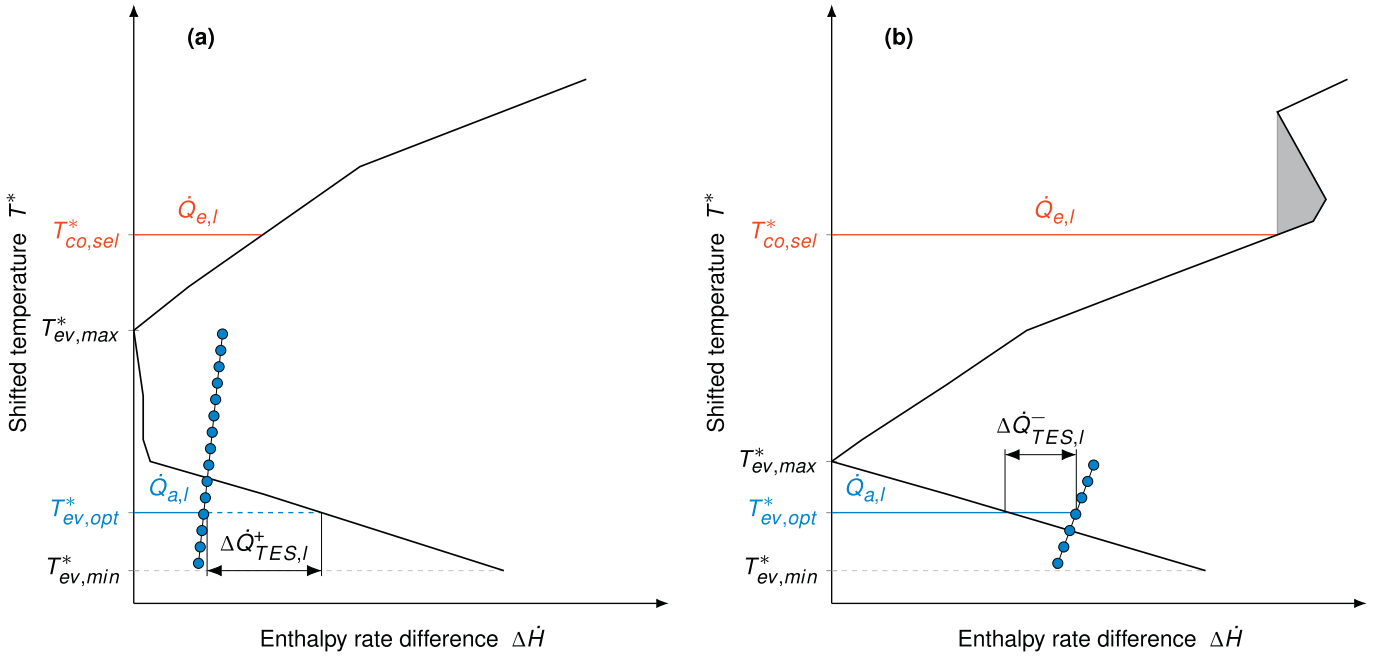

Fig. 2. GCC of two TSs including the emitted heat flow $\dot{Q}_{e,l}$ by the condenser, the absorbed heat flow by the evaporator $\dot{Q}_{a,l}$, and the COP Curves (blue dotted curve) for the identification of the optimal shifted evaporator temperature $T^*_{ev,opt}$. Fig. 2 (a) represents a TS with a higher cooling demand than the HP can provide (the heat surplus from the process $\Delta\dot{Q}^+_{TES,l}$ has to be transferred to a storage) and Fig. 2 (b) represents a TS with a lower cooling demand than the HP can provide (the heat deficit of the process $\Delta\dot{Q}^-_{TES,l}$ has to be provided by a storage to the HP). (For interpretation of the references to colour in this figure legend, the reader is referred to the Web version of this article.)

thermo-economic optimization.

2.5. Step 5 – design of heat exchanger network

The HEN design is performed using insight based methods as well. Therefore, the Pinch Design Rules presented by Linnhoff and Hindmarsh [32] are used to create the HEN. By using the commercial software SuperTarget™ it is allowed to relax these rules within the design process. For inter-plant heat recovery additional HRLs are added to ensure the flexibility of the individual processes.

2.6. Step 6 – thermo-economic optimization

After step 5, the HEN structure is defined. To avoid the unrealistic large approach temperatures in the condenser and evaporator, a thermo-economic optimization is performed. Thereby, temperature levels for the condensation, the evaporation, and the HRLs are optimization variables. In addition, loading and unloading profiles of both storages are determined. As the objective, the total annual costs (TAC) are minimized, resulting in an NLP formulation. In Fig. 4, the superstructure of the HP-HRL system is shown.

2.6.1. Formulation of objective function: total annual costs minimization

As objective function, the TAC are minimized by

$$\mathrm{TAC} = \min\left(C_{inv,a} + C_{op,a}\right) \tag{10}$$

where $C_{inv,a}$ represents the annual investment costs and is estimated by the sum of all equipment costs C_E and annualized using the interest rate i_r and the investment period n as follows:

$$C_{inv,a} = \frac{i_r\,(1+i_r)^n}{(1+i_r)^n - 1}\sum_E C_E \tag{11}$$

The equipment costs are estimated using factorial methods. To calculate the investment costs of an equipment, main plant item costs $\mathrm{MPIC_E}$ are multiplied by Lang factors F_E [33] as follows:

$$C_E = F_E\,\frac{I_{PMEI2}}{I_{PMEI1}}\mathrm{MPIC_E} \tag{12}$$

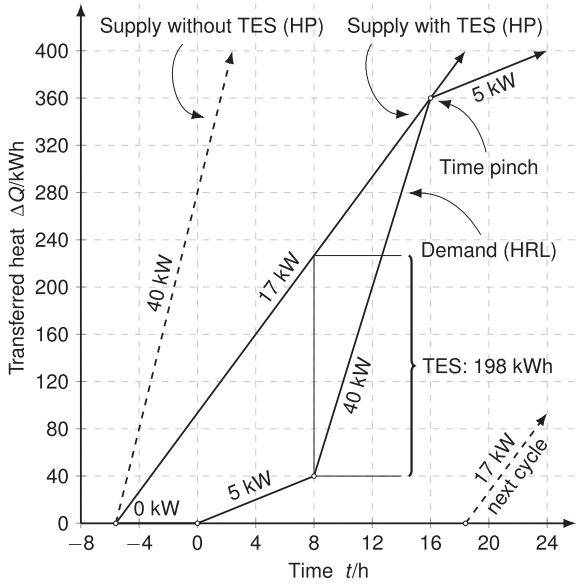

Fig. 3. Supply & Demand Curves in $\Delta Q, t$-chart for optimum sizing of HP-HRL system.

The Lang factor includes installation, piping, control system, building, site preparation, and service facility costs. To consider inflation and deflation, the cost function is adjusted using the plant, machinery, equipment group index I_{PMEI} of the capital goods price index [34]. For an equipment, the $\mathrm{MPIC_E}$ is defined by

$$\mathrm{MPIC_E} = C_{E,0} + C_{E,1}\,Q^{f_{E,d,1}} + C_{E,2}\,Q^{f_{E,d,2}} \tag{13}$$

where Q represents the capacity of the equipment such as its area A for a HEX and $f_{E,d}$ the degression factor. With

$$C_{HP-\mathrm{HRL}} = C_{comp}(P_i) + C_{en}(P_{el}) + C_{co}(A_{co}) + C_{ev}(A_{ev}) + C_{TES,H}(V_{TES,H}) + C_{TES,C}(V_{TES,C}) \tag{14}$$

the module cost for the HP-HRL system $C_{HP-\mathrm{HRL}}$ is estimated by summation of the individual equipment costs of the HP (compressor C_{comp}, engine C_{en}, condenser C_{co}, evaporator C_{ev}, hot TES $C_{TES,H}$ and cold TES $C_{TES,C}$). The annual operating cost is given by

$$C_{op,a} = d_a \sum_{l=1}^{L}\left(\dot{Q}_m\,c_m + \dot{Q}_n\,c_n + P_{el}\,c_{el}\right)\Delta t_l \tag{15}$$

where d_a represents the annual operating days, $\dot{Q}$, the needed hot utility (HU, m) and cold utility (CU, n), c their corresponding specific cost, P_{el} the constant electrical power demand by the compressor, and c_{el} the specific electricity cost.

2.6.2. Formulation of heat transfer

The area for a HEX, which is the driving force for its costs is defined by

$$A_s = \max_l\left(\frac{\dot{Q}_{s,l}}{U_s\,LMTD_{s,l}}\right)\ \forall s \tag{16}$$

where the subscript s represents either a hot i or cold j process stream. By the use of Chen's approximation [35], the logarithmic mean temperature difference (LMTD) in HEX is estimated by

$$LMTD_{s,l} \approx \left(\Delta T_1\,\Delta T_2\left(\frac{\Delta T_1 + \Delta T_2}{2}\right)\right)^{1/3}. \tag{17}$$

In contrast to the exact formulation, using this Chen's approximation has the advantage that the singularity problem of the LMTD arising if $\Delta T_1 = \Delta T_2$ is omitted. The resulting LMTD is slightly underestimated, and thus the HEX area and its costs is slightly overestimated. For all HEX between hot process streams and the HRL ($s = i$), the temperature differences are given by

$$\Delta T_1 = T_{i,l,S} - T_{C,h} \qquad \forall i,\ \forall l \tag{18}$$

$$\Delta T_2 = T_{i,l,T} - T_{C,c} \qquad \forall i,\ \forall l \tag{19}$$

where $T_{i,l,S}$ and $T_{i,l,T}$ represent the supply and the target temperature of the relating hot process stream. The hot and cold layer temperatures of the cold storage (C) are given by $T_{C,h}$ and $T_{C,c}$. For all HEX between cold process streams and the HRL ($s = j$), the temperature differences are given by

$$\Delta T_1 = T_{H,h} - T_{j,l,T} \qquad \forall j,\ \forall l \tag{20}$$

$$\Delta T_2 = T_{H,c} - T_{j,l,S} \qquad \forall j,\ \forall l \tag{21}$$

whereby $T_{H,h}$ and $T_{H,c}$ represent the hot and cold layer

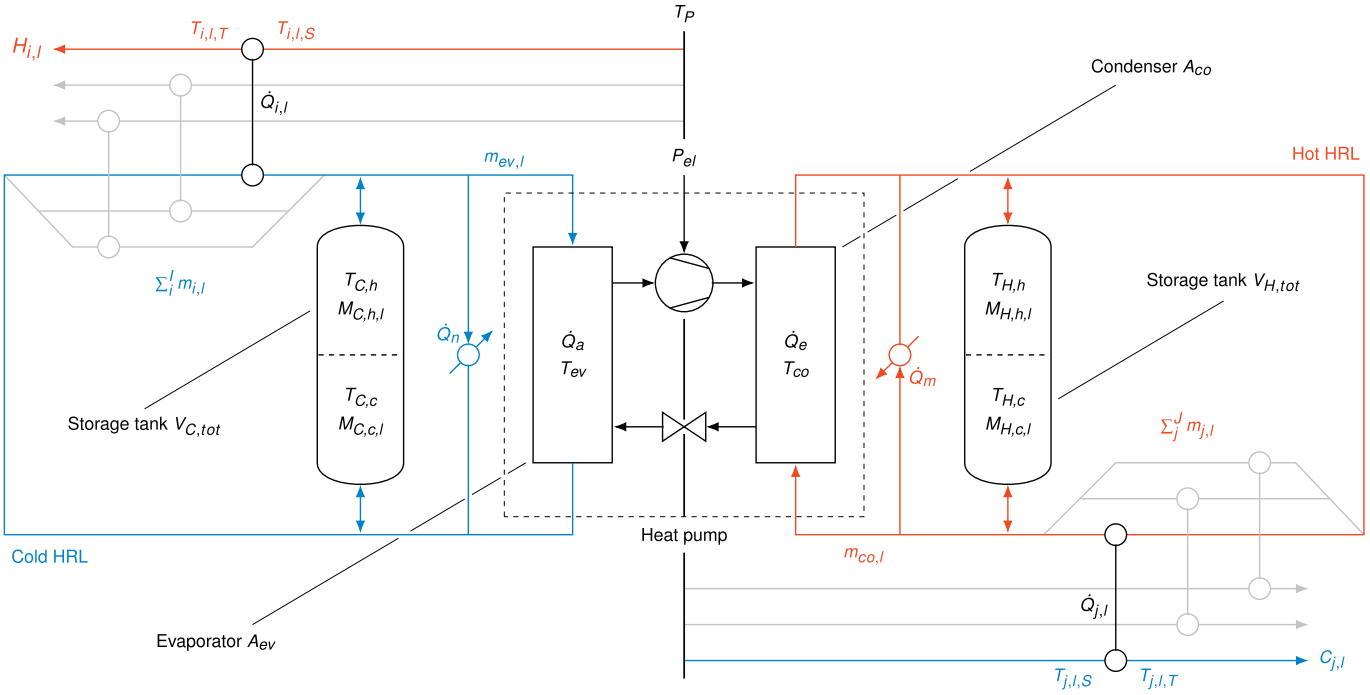

Fig. 4. Superstructure HP-HRL system.

temperatures of the hot storage (H). The overall heat transfer coefficient is defined by

$$\frac{1}{U_{s,HRL}} = \frac{1}{h_s} + \frac{1}{h_{HRL}} \qquad \forall s. \tag{22}$$

To guarantee feasible heat transfer below the pinch (see Fig. 4), the supply, as well as the target temperature of the hot process streams, have to be higher than the associate storage layer temperatures of the cold storage which is given by

$$T_{i,l,S} \geq T_{C,h} \qquad \forall i,\ \forall l \tag{23}$$

$$T_{i,l,T} \geq T_{C,c} \qquad \forall i,\ \forall l. \tag{24}$$

Feasible heat transfer above the pinch is ensured by

$$T_{j,l,T} \leq T_{H,h} \qquad \forall j,\ \forall l \tag{25}$$

$$T_{j,l,S} \leq T_{H,c} \qquad \forall j,\ \forall l \tag{26}$$

where the supply and target temperatures of the process streams have to be lower than the associated layer temperature of the hot TES. Heat transfer between HRLs and HP are guaranteed by

$$T_{C,h} \geq T_{C,c} \geq T_{ev} \tag{27}$$

$$T_{co} \geq T_{H,h} \geq T_{H,c} \tag{28}$$

where the temperature level of evaporation has always to be lower than the temperatures of the cold storage as well as the temperature level of the condensation always has to be higher than the temperatures of the hot storage.

2.6.3. Formulation of heat recovery loop

The needed storage volume which is the driving force for its costs is given by

$$V_{C,tot} = \frac{M_{C,h,l} + M_{C,c,l}}{\rho_{HRL}} \qquad \text{for } l = 1 \tag{29}$$

$$V_{H,tot} = \frac{M_{H,h,l} + M_{H,c,l}}{\rho_{HRL}} \qquad \text{for } l = 1 \tag{30}$$

where M represents the mass inventory of the related temperature layer in the storage and ρ_{HRL} the density of the storage media. The total mass inventory is constant over time and therefore only needs to be defined for the first TS ($l = 1$). With

$$M_{C,h,l+1} = M_{C,h,l} + \sum_{i=1}^{I} (m_{i,l}) - m_{ev,l} \qquad \forall l \tag{31}$$

$$M_{C,c,l+1} = M_{C,c,l} - \sum_{i=1}^{I} (m_{i,l}) + m_{ev,l} \qquad \forall l \tag{32}$$

$$M_{H,h,l+1} = M_{H,h,l} - \sum_{j=1}^{J} \left(m_{j,l}\right) + m_{co,l} \qquad \forall l \tag{33}$$

$$M_{H,c,l+1} = M_{H,c,l} + \sum_{j=1}^{J} \left(m_{j,l}\right) - m_{co,l} \qquad \forall l \tag{34}$$

the mass balance for both HRLs is applied, whereby with

$$M_{C,h,l} \geq 0\, M_{C,c,l} \geq 0 \qquad \forall l \tag{35}$$

$$M_{H,h,l} \geq 0\, M_{H,c,l} \geq 0 \qquad \forall l \tag{36}$$

it is ensured that the mass inventory is never negative. The mass which has to be transferred in each TS to cover the heating and cooling demand is defined by

$$m_{i,l} = \frac{\dot{Q}_{i,l}\,\Delta t_l}{c_{p,HRL}(T_{C,h} - T_{C,c})} \qquad \forall i,\ \forall l \tag{37}$$

$$m_{j,l} = \frac{\dot{Q}_{j,l}\,\Delta t_l}{c_{p,HRL}(T_{H,h} - T_{H,c})} \qquad \forall j,\ \forall l \tag{38}$$

where $c_{p,HRL}$ is the specific heat capacity of the storage media. Further with

$$m_{ev,l} = \Delta t_l\,\dot{m}_{ev} = \frac{\Delta t_l}{\sum_{l=1}^{L}\Delta t_l}\sum_{i=1}^{I}\sum_{l=1}^{L} m_{i,l} \qquad \forall l \tag{39}$$

$$m_{co,l} = \Delta t_l\,\dot{m}_{co} = \frac{\Delta t_l}{\sum_{l=1}^{L}\Delta t_l}\sum_{j=1}^{J}\sum_{l=1}^{L} m_{j,l} \qquad \forall l, \tag{40}$$

the transferred mass through evaporator and condenser is given.

2.6.4. Formulation of heat pump cycle

The resulting heat flow which is absorbed by the evaporator of the HP is determined by fulfilling the energy balance of the cold HRL given by

$$\dot{Q}_{C,HRL} = \dot{Q}_a + \dot{Q}_n = \dot{m}_{ev}\,c_{p,HRL}\,(T_{C,h} - T_{C,c}) \tag{41}$$

where $\dot{Q}_n$ represents rebalancing CU which is needed if the temperature lift ΔT_{lift} is increased in the optimization and thus the absorbed heat flow $\dot{Q}_a$ is smaller than the cooling demand of the process. The emitted heat flow by the condenser is determined by fulfilling the energy balance of the hot HRL given by

$$\dot{Q}_{H,HRL} = \dot{Q}_e + \dot{Q}_m = \dot{m}_{co}\,c_{p,HRL}\,(T_{H,h} - T_{H,c}) \tag{42}$$

where $\dot{Q}_m$ is the rebalancing HU which is needed if the temperature lift is decreased in the optimization and thus the emitted heat flow $\dot{Q}_e$ is smaller than the heating demand of the process. By

$$\mathrm{COP} = \zeta\,\frac{T_{co}}{T_{co} - T_{ev}} = \frac{\dot{Q}_e}{P_{el}} \tag{43}$$

the HP cycle is approximated using the 2^{nd} law efficiency. With the energy balance of the HP

$$\dot{Q}_e = \dot{Q}_a + P_{el}\,\eta_{drive} = \dot{Q}_a + P_i \tag{44}$$

the resulting electrical power demand of the HP is given which is the driving force for the compressor and engine costs.

2.7. Step 7 – calculation of greenhouse gas emissions

Using the resulting electrical power and utility demand with

$$\mathrm{CO_2}e_a = d_a\sum_{l=1}^{L}\left(\dot{Q}_m\,\xi_m + \dot{Q}_n\,\xi_n + P_{el}\,\xi_{el}\right)\Delta t_l \tag{45}$$

the annual greenhouse gas emissions are determined.

3. Case study: butter production on a dairy site

3.1. Process description

The analyzed process represents two plants which are used for producing raw materials for butter production on a large dairy site. The first plant produces anhydrous milk fat (AMF) and the second plant is used for cream treatment (CT). Fig. 5 (a) and Fig. 5 (b) are showing the state-of-the-art how such plants are usually designed. Further, the cleaning-in-place (CIP) system for both plants is included in the analysis (Fig. 5 (c)).

AMF is almost pure milk fat (99.0 – 99.95 %). During its production, buttermilk (0.24 %) and beta serum (2.00 %) are produced as by-products. The main task of this process is the separation of the oil-in-water emulsion (cream).

In a first step, the cream is heated from 8 °C to 68 °C and concentrated in the cream concentrator to 72.00 %. In the homogenizer, mechanical energy is used to produce smaller oil globules by breaking the surface tension. After this procedure, the fat content is increased by separation in the oil concentrator to 90.00 %. The resulting oil is heated to 95 °C for pasteurization purposes. For refining purposes, the oil is washed with water in the polisher. Thereby, the water is added at the same temperature as the oil. This procedure removes water-soluble substances such as proteins. Thereby, the oil concentration is increased to 99.00 %. For final refining, the oil is fed to the deodorizer. By stripping the oil with steam, disruptive aromas, odors, free fatty acids, and other minor impurities are removed. Finally, the resulting AMF with a concentration of 99.90 – 99.95 % is cooled to 40 °C.

For the by-product buttermilk, the fat content in the side stream of the cream concentrator is further reduced in the buttermilk separator from 0.33% to 0.24%. In a next step, the buttermilk is thermalized by heating to 80 °C. Finally, the buttermilk is cooled to 8 °C.

The side stream of the oil concentrator and the buttermilk separator are collected and fed to the beta serum separator. As a result, beta serum with a concentration of 2.00 % and oil with a concentration of 41.00 % is produced. The beta serum is cooled to 8 °C, and the oil is fed back to the oil concentrator. In the CT plant, cream with a fat mass fraction of 40 % is pasteurized. Further, by using a spinning cone column (SCC), undesired flavors are removed from the cream. Finally, the cream is cooled to the starting temperature. Heat recovery (HR) is achieved by using an intermediate hot water loop.

After production, both plants must be cleaned. A CIP system is installed for this purpose. The advantage of such systems is that they do not require disassembly before cleaning. In order to provide the needed hot rinse water, an alkaline solution, nitric acid, and cold rinse water, tanks are installed as shown in Fig. 5 (c). The following procedure is applied to clean the plant [39]:

1. Pre-Rinsing with hot water at 50 °C for 10 min
2. Circulation of an alkaline detergent solution (1.00 %) at 75 °C for 30 min
3. Rinsing out of alkaline detergent solution with hot water at 50 °C for 5 min
4. Circulation of nitric acid (1.50 %) at 70 °C for 20 min
5. Post-Rising with cold water at 15 °C for 15 min

To clean the plant, the CIP system requires a mass flow of $\dot{m} = 6.53$ kg/s for the AMF production plant and a mass flow of $\dot{m} = 1.80$ kg/s for the CT plant. Thereby, the cleaning fluids are heated up over the whole process duration using utilities.

As utility, steam produced in a natural gas boiler and chilled

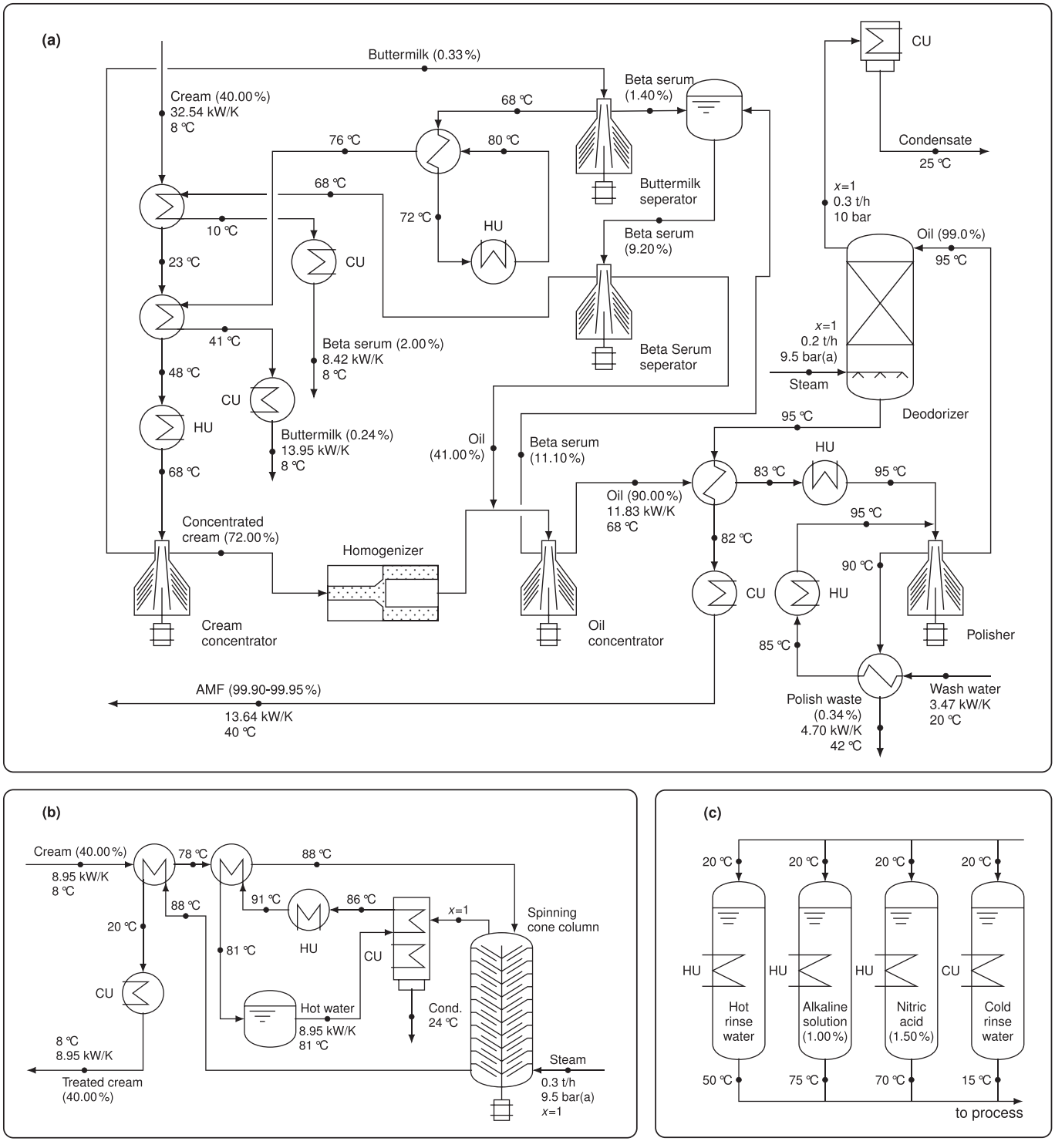

Fig. 5. Flowcharts of typical design of analyzed dairy processes: (a) AMF production plant, (b) CT plant, (c) CIP system.

water (−5 °C–0 °C) produced in a refrigerator unit are used. In Table 1, the process stream data is given. Thereby, the process streams are assigned to the respective process. In Table 2, the used utilities including their price, greenhouse gas (GHG) emissions as well as the additional CO_2 levy are listed whereby the levy for electricity is already included in its price. In Table 3, the cost factors for used equipment are listed. Thereby, the correction using Lang factors F_E, index ratios I_{PMEI}, material f_m, and pressure factors f_p are already applied to the cost factors C_0, C_1, and C_2. As amortization parameters, an investment period of 12 years and an interest rate of 7% is given.

3.2. Integration of heat pump and heat recovery loop system

Using the Time Slice Model, five TSs per day can be identified. Although only TS_2-TS_4 have heating and cooling demand. TS_1 and TS_5 are still considered giving the heat pump (HP)-heat recovery loop (HRL) system the possibility to continue operating and store or release heat from the HP in both thermal energy storages (TESs). The energy targets are determined in a next step using an overall ΔT_{min} of 10 K for each TS. In Fig. 6, the heating and cooling requirement, resulting in Grand Composite Curves (GCCs) of TS_2 to TS_4, are shown.

The selected overall initial condensation temperature is determined by searching for the highest possible HR with a small as possible temperature lift ΔT_{lift}.

Thus, no self-sufficient pockets are allowed to be destroyed a shifted overall condensation temperature of $T^*_{co,sel} = 33.8°C$ is selected. The corresponding optimal shifted overall evaporator temperature is $T^*_{ev,opt} = 8.3°C$. Yielding Supply & Demand Curves are shown in Fig. 7. It is conclude that by the integration of two storages, one with 0.68 MWh to support the evaporator of the HP and another one with 1.35 MWh to support the condenser of the HP, heat flow demand can be reduced by around two thirds.

The optimal temperatures of condensation, evaporation, and temperatures of the storage layers found by the thermo-economic optimization are shown in Fig. 8. Due to the optimization of the temperature levels, an additional rebalancing hot utility (HU) is needed to compensate for the reduced emitted heat flow by the HP caused by the lower temperature lift.

3.3. Total Site Heat Integration

To optimize the overall process, a Total Site Heat Integration (TSHI) approach using HRLs for inter-plant HR is chosen due to the following reasons:

- By designing a heat exchanger network (HEN) for each plant separately, the plants are not depending on each other. During downtimes or maintenance of one plant, the others are able to run independently.
- By designing separate HENs for each plant thus the continuous intra-plant operation, just the HRLs have to deal with the non-continuous behavior of the process.

In the GCCs of the single plants, it can be seen (Fig. 9), that due to the integration of the HP-HRL system a pocket in the AMF production plant is destroyed (see Fig. 9 (a)) which would increase the cold utility (CU) demand. As a result of this, a low-temperature hot water (LTHW)-HRL with a temperature range of 62-40 °C is needed which transfers heat from the AMF production plant to the CIP system. Further inter-plant HR is achieved using a high-temperature hot water (HTHW)-HRL with a temperature range of 98-70 °C as shown in the Fig. 9.

The HTHW-HRL is used to reduce the HU demand for the AMF production and the CIP system. Due to the fact that their heating demand is higher than the supplied heat from the CT process, there is an additional HU need which is supplied from a hot water boiler.

4. Results and discussion

To evaluate the time-wise process decoupling, in Fig. 10, the

Table 1
Process requirements.

Stream	#	T_S	T_T	CP	$\Delta\dot{H}$	ΔH	h	t_{start}	t_{end}
	–	°C	°C	kW / K	kW	kWh	W / (m² K)	h	h
AMF production									
Cream heating	C_3	8	68	32.54	1952.4	14643	500	10	17.5
Oil pasteurization	C_4	68	95	11.83	319.41	2395.58	500	10	17.5
AMF cooling	H_3	95	40	13.64	750.2	5626.5	500	10	17.5
Buttermilk thermalization	C_5	68	80	13.95	167.4	1255.5	500	10	17.5
Buttermilk cooling	H_4	80	8	13.95	1004.4	7533	500	10	17.5
Beta Serum cooling	H_5	68	8	8.42	505.2	3789	500	10	17.5
Wash water heating	C_6	20	90	3.47	260.25	1951.88	2000	10	17.5
Polish waste cooling	H_6	90	42	4.7	225.6	1692	500	10	17.5
Deodorizer evaporation a	$C_{7,a}$	25	177.67	0.27	41.22	309.15	2000	10	17.5
Deodorizer evaporation b	$C_{7,b}$	177.67	178.67	114.27	114.27	857.03	5000	10	17.5
Deodorizer condensation a	$H_{7,a}$	178.67	177.67	171.38	171.38	1285.35	5000	10	17.5
Deodorizer condensation b	$H_{7,b}$	177.67	25	0.41	62.59	469.43	2000	10	17.5
Cream treatment									
Cream pasteurization	C_1	8	88	8.95	716	5370	500	8	15.5
Treated cream cooling	H_1	88	8	8.95	716	5370	500	8	15.5
SCC evaporation a	$C_{2,a}$	24	177.67	0.41	63	472.50	2000	8	15.5
SCC evaporation b	$C_{2,b}$	177.67	178.67	171.38	171.38	1285.35	5000	8	15.5
SCC condensation a	$H_{2,a}$	178.67	177.67	171.38	171.38	1285.35	5000	8	15.5
SCC condensation b	$H_{2,b}$	177.67	24	0.41	63	472.50	2000	8	15.5
CIP system									
Pre-rinse water	C_8	20	50	0.92	27.58	262.01	2000	8	17.5
Alkaline detergent solution	C_9	20	75	1.84	101.20	961.40	2000	8	17.5
Nitric acid	C_{10}	20	70	1.23	61.50	584.25	2000	8	17.5
Post-rinse water	H_8	20	15	0.92	4.6	43.7	2000	8	17.5

Table 2
Utility data[a].

Utility	T_{in} °C	T_{out} °C	h W/(m²K)	c^{***}_{day} NZD/MWh	c^{***}_{night} NZD/MWh	ξ t_{CO2e}/MWh	c_{CO2} NZD/$t_{CO2}e$	c_{CO2} NZD/MWh
Steam	190	189	5000	50	50	0.21	20	4.2
Hot water*	100	95	2000	50	50	0.21	20	4.2
Chilled water**	−5	0	2000	34	27	0.04	–	0.8
Electricity	–	–	–	100	80	0.13	–	2.6

* Natural gas boiler (η = 0.9)/ ** Refrigerator unit (COP = 2.98)/ *** Day: 05:00–23:00/Night: 23:00–05:00.
[a] Natural gas costs: MBIE [36]/Electricity costs: Em6 [37]/GHG emissions: EECA [38].

Table 3
Equipment costs data with an uncertainty of ±30% [40].

Equipment	F_E	I^*_{PMEI04}	I^*_{PMEI17}	Q	$C_0/10^3$	$C_1/10^3$	$f_{d,1}$	C_2	$f_{d,2}$
Stainless steel plate HEX	2.91	1093	1201	A (m²)	4.35	0.66	1	–	–
Reciprocal piston compressor	3.24	1070	1432	P_i (kW)	42.28	5.94	1	4.09	2
Variable speed driver motor	3.20	1044	1249	P_{el} (kW)	4.02	0.49	1	–	–
Storage vessel	3.20	1157	1724	V (m³)	–	1.53	0.597	–	–
Refrigeration unit	3.24	1070	1432	$\dot{Q}_{CU}$ (kW)	–	11.32	0.806	–	–
Natural gas steam boiler 12.5 bar (a)	2.24	1180	1395	$\dot{Q}_{HU}$ (kW)	–	1.06	0.805	–	–
Natural Gas water boiler	2.24	1180	1395	$\dot{Q}_{HU}$ (kW)	13.21	0.14	1	–	–

* Index data provided by Stats NZ [34].

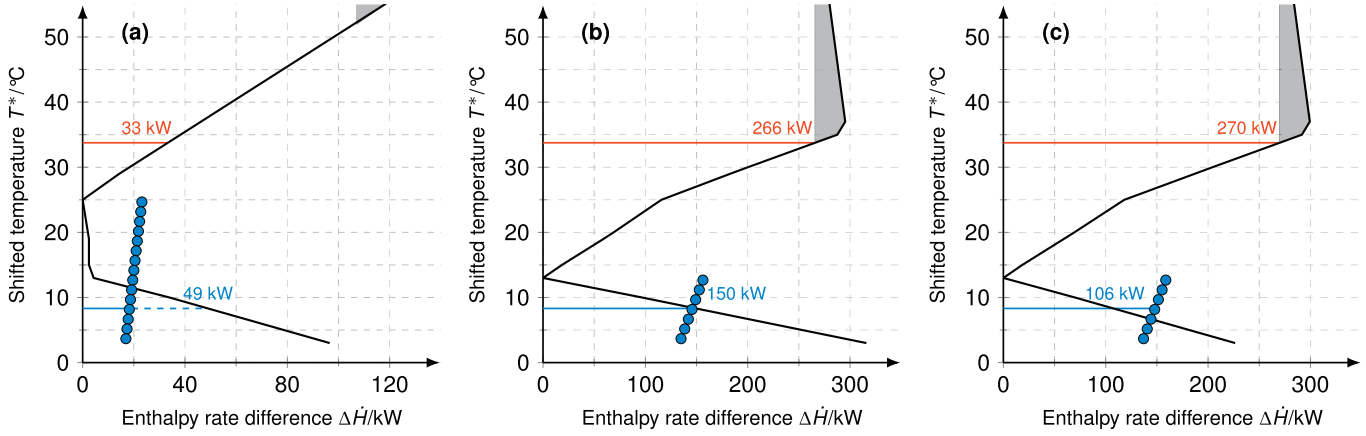

Fig. 6. Sections of the GCC of the total site with COP Curves, resulting absorbed and emitted heat flow by the HP: (a) TS_2: 8–10 h, (b) TS_3: 10–15.5 h, and (c) TS_4: 15.5–17.5 h.

annualized costs of the HP-HRL system are plotted as a function of the daily operating hours of the HP. It is important to notice that the daily energy supplied by the HP-HRL system does not change as a result of the reduction in the daily operating time. Reducing the operating hours of the HP does not influence the utility demand. Therefore, utility costs are not displayed in Fig. 10.

In Fig. 10, it can be seen, that the annualized costs of the HP-HRL system is minimized at a daily operation duration of 24 h. Thereby, the main driver is the compressor size which is increased by providing the same daily energy within a reduced operation time.

In a next step, the new hybrid method is compared with the not optimized plant, the optimized plant using the described TSHI approach, and the existing insight based method [25]. Therefore, it is important to mention, that the thermo-economic optimization only influences the HP-HRL system and thus not a large improvement for overall total annual costs (TAC) is expected. However, by optimizing the storage temperatures as well as the condenser and evaporator temperatures, realistic approximate temperatures are obtained in condenser $\Delta T_{co,apr}$ and evaporator $\Delta T_{ev,apr}$ with a reduced temperature lift for HP ΔT_{lift} shown in Table 4.

For an economic evaluation the methods are compared with the not optimized process on the dairy site (see flowchart in Fig. 5) and the TSHI approach. The optimized HENs are designed using the software SuperTarget™ and are provided in the Appendix. To ensure a common base for comparison, the optimized HEN is modified as little as possible to integrate the HP-HRL system. Resulting utility demand, corresponding GHG emissions, and the costs for each method are shown in Table 5. Further, in Table 6 the resulting investment costs are compared.

It can be seen that already the TSHI approach is resulting in a reduction of operating costs by 61% and 52% in GHG emission. By using the insight based method for the integration of the HP-HRL

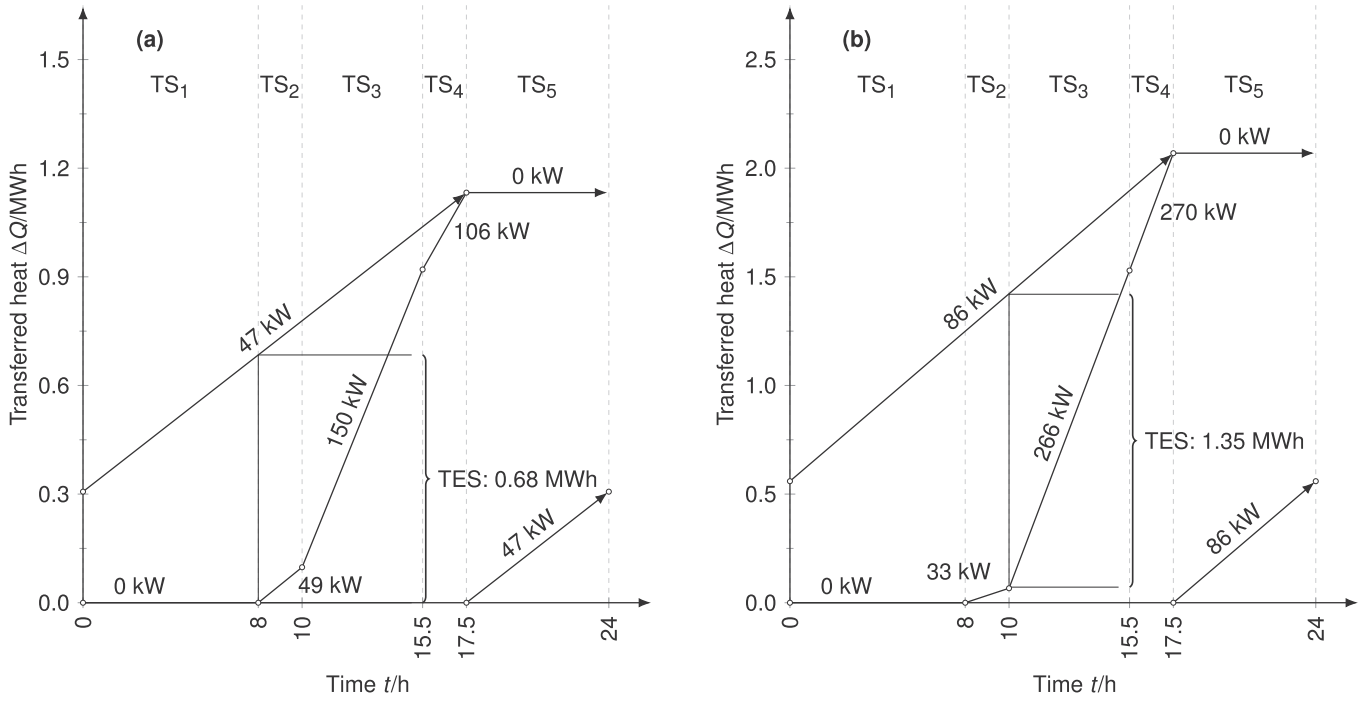

Fig. 7. Supply & Demand Curves for: (a) cold HRL $\dot{Q}_{C,HRL}$ and (b) hot HRL $\dot{Q}_{H,HRL}$

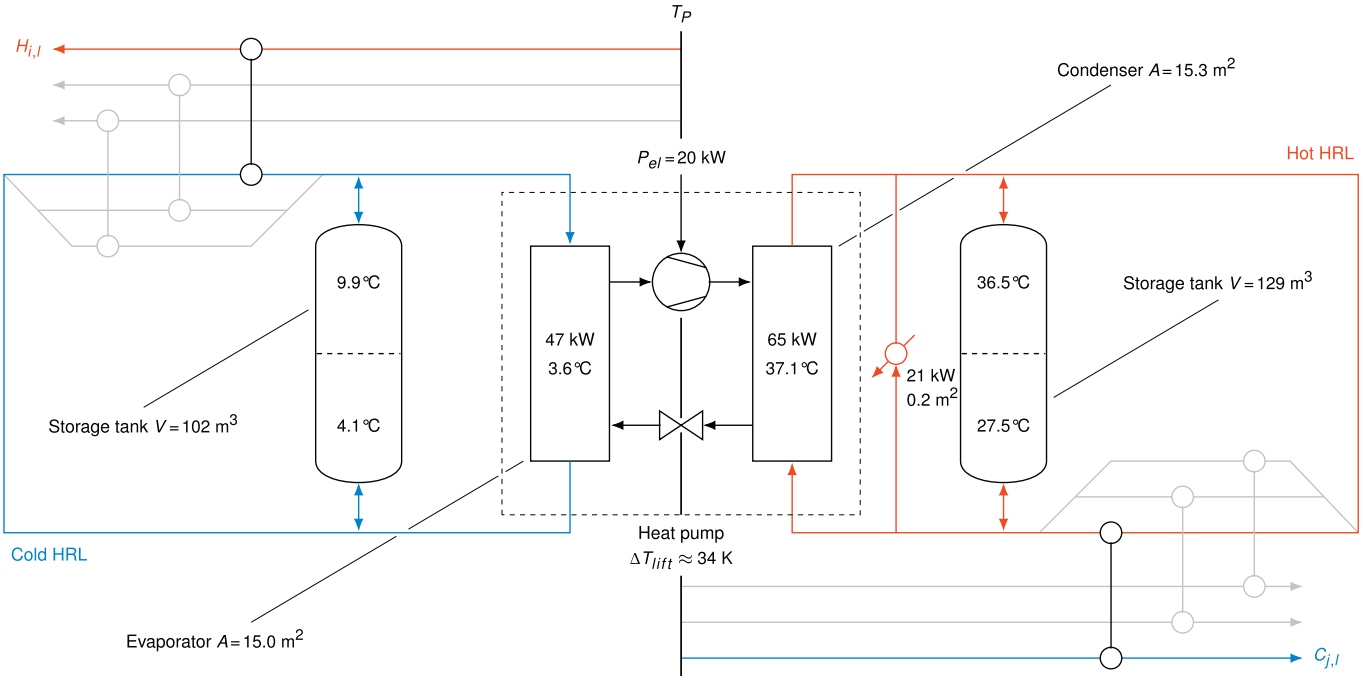

Fig. 8. Resulting HP-HRL system.

system, operating costs and GHG emissions are reduced further by 66% and 65%. The hybrid method operating costs are slightly more reduced by 68%. In contrast to this, GHG emissions are only reduced by 63%. The higher GHG emissions are caused by the utility rebalancing needed due to the smaller temperature lift of the HP. Since GHG emissions are not a objective in the optimization, there is no tradeoff between temperature lift and needed rebalancing utility.

By the reduction of operating costs, investment costs are increased due to the usual tradeoff between them (see Table 6). By using the hybrid instead of the insight based method, investment cost for the HP-HRL system are reduced by 29%. Due to smaller temperature differences in heat exchanger (HEX) connected to the

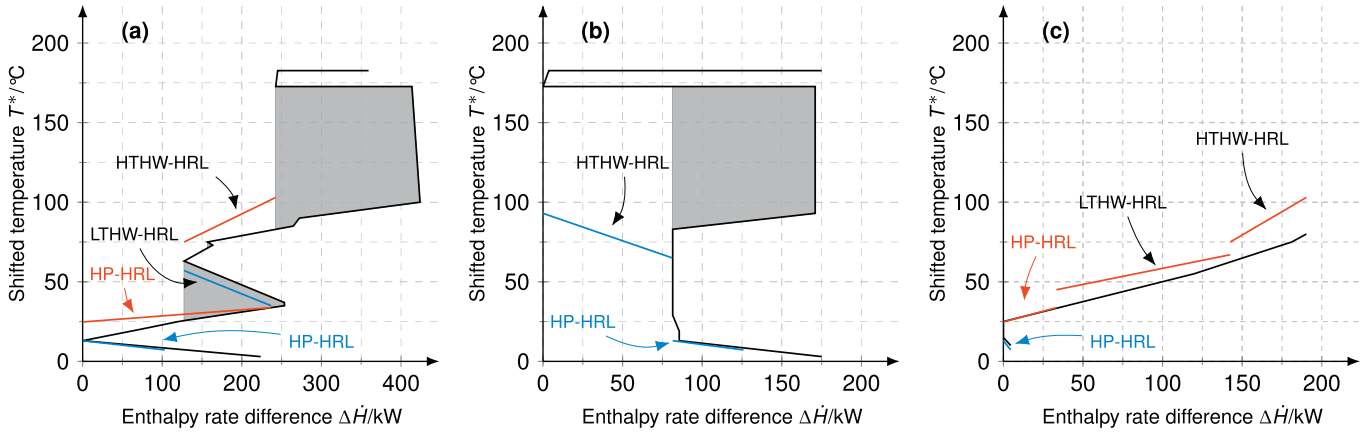

Fig. 9. GCCs of the plants including heat flows of the HP-HRL system, the LTHW-HRL, and the HTHW-HRL: (a) AMF production plant (TS_3 and TS_4), (b) CT plant (TS_3 to TS_4), and (c) CIP system (TS_2 to TS_4).

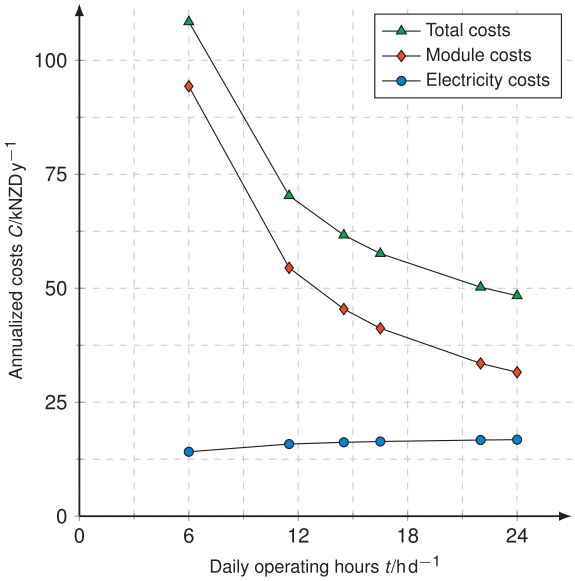

Fig. 10. Annualized costs for the HP-HRL system excluding operating costs for HU and CU.

Table 4
Comparison of temperature differences for different methods.

Temperature difference (K)	Insight based method	Hybrid method
$\Delta T_{co,apr}$	7.1	0.6
$\Delta T_{ev,apr}$	7.9	0.5
ΔT_{lift}	51.4	33.5

HP-HRL system costs for the different HEN designs are increased. Further due to the utility rebalancing a larger water boiler is needed.

TAC (rounded values) are reduced using the TSHI approach from 598, 000 NZD /y to 430, 000 NZD /y. By the use of the insight based method TAC can be further reduced to 413, 000 NZD /y and with the hybrid method slightly more to 412, 000 NZD /y.

The resulting operating costs are strongly depended on the natural gas and electricity price. In order to analyze their influence, a sensitivity analysis is performed to show for which natural gas and electricity prices it is most beneficial to optimize the process and when to integrate the HP-HRL system. In Fig. 11 the results are shown as regions for each option, where the corresponding TAC are the lowest compared to the other designs. Thereby, an uncertainty of 30% for investment costs is considered (dotted and dashed line). It can be seen that the not optimized process is not competitive for realistic natural gas and electricity price.

The actual price range is clearly in the region where it is most beneficial to optimize the process as well as integrating the HP-HRL system. Future price trends are predicted to tend to a larger price increase for natural gas than for electricity. Therefore, in the future the integration of a HP-HRL system tends to become even more beneficial.

The goal of not being expensive in terms of computing time and resources is achieved by solving the NLP formulation within an average computing time of 0.303 s over 30 runs of the optimization solver Ipopt (Interior point optimizer) 3.12.4 [41] on an Intel Core i7-7600U processor and 16 GB RAM.

By its application on the dairy site case study, the method has proven its practicality. Thus the manual HEN design, the decisions if a process stream should be connected to the HP-HRL system or not is up to the experienced engineer, which increases the flexibility by the application of the method. Further, optimal results regarding the

Table 5
Comparison of utility demand of the different optimization approaches.

Utilty type	Not optimized			Total Site Heat Integration			Insight based method			Hybrid method		
	MWh/y	t_{CO2}/y	NZD/y	MWh/y	t_{CO2}/y	NZD/y	MWh/y	t_{CO2}/y	NZD/y	MWh/y	t_{CO2}/y	NZD/y
Steam	3495	734	187468	799	168	42842	799	168	42842	799	168	42842
Hot water	0	0	0	1101	231	59069	397	83	21311	579	122	31042
Chilled water	4344	174	147701	885	35	28545	554	22	17867	554	22	17867
Electricity	0	0	0	0	0	0	933	44	32363	177	23	16789
Total		908	335169		434	130456		317	114383		335	108540

Table 6
Comparison of investment costs (NZD) for the different optimization approaches.

Investment (NZD)	Not optimized	Total Site Heat Integration	Insight based method	Hybrid method
HEN CT	237790	217482	224916	226242
HEN AMF	397395	747345	876433	906887
HEN CIP	18170	21312	54704	55791
HEN HTHW	0	28784	25589	25589
HEN LTHW	0	0	8754	8754
Steam boiler	261726	101931	101931	101931
Water boiler	0	73284	28252	31126
HP-HRL	0	0	351679	250817
Refrigerator unit	1170707	1189009	802934	802934
Total investment costs	2085788	2379147	2466192	2410071

reduced search space are obtained with short computation times.

In the method, an overall condensation and evaporation temperature for all TSs is chosen having a total time-wise decoupling of the HP. Therefore, it is possible for the HP to operate continuously without changing the operation condition for the compressor. Thus the compressor can operate at its design point having the highest efficiency. For the analyzed case study, which has a change in the pinch temperature over time of 12 K, this approach applies well. However, if the change of the pinch temperature over time increases, the presented method will lead to a larger temperature lift for the HP, which reduces the efficiency of the HP. Therefore, the current approach does not apply well to processes with extensive changes in the pinch temperature over time.

5. Conclusions

Applying the hybrid insight based and mathematical programming approach to a non-continuous dairy site showed, that the time-wise process decoupling of the heat pump (HP) is successful in terms of greenhouse gas (GHG) emissions and total annual costs (TAC) reduction. By comparing the results on a global perspective the ratio of electrical price to natural gas price is a good indicator. The actual ratio in New Zealand is $c_{el}/c_{NG} = 1.7$. With a ratio of 1.3 in Switzerland [8], the integration of a HP-HRL into dairy process tends to be even more beneficial. In contrast to this, in many other industrial nations such as Germany, a large proportion of industry do not have a renewable energy levy that has led to a ratio between 2 and 3 [42] resulting in the integration of a HP-HRL system into a dairy process being less beneficial.

By using the hybrid method instead of the insight based method TAC is just slightly more reduced and GHG emission even increased. Nevertheless, the hybrid method achieves realistic approach temperatures in condenser and evaporator in contrast to the insight based method. The increased GHG emissions are caused by the utility rebalancing in the HP-HRL system. In some cases, it is possible to integrate the needed rebelancing duty back into the process for further utility reduction. This is not possible for the analyzed case study.

By extending the insight based approach with the nonlinear programming formulation high flexibility in the application of the method is preserved and execution time for the method is just increased slightly. In terms of project costs, both the insight based and the sophisticated mathematical programming method require engineers with experience in their field, either insight based

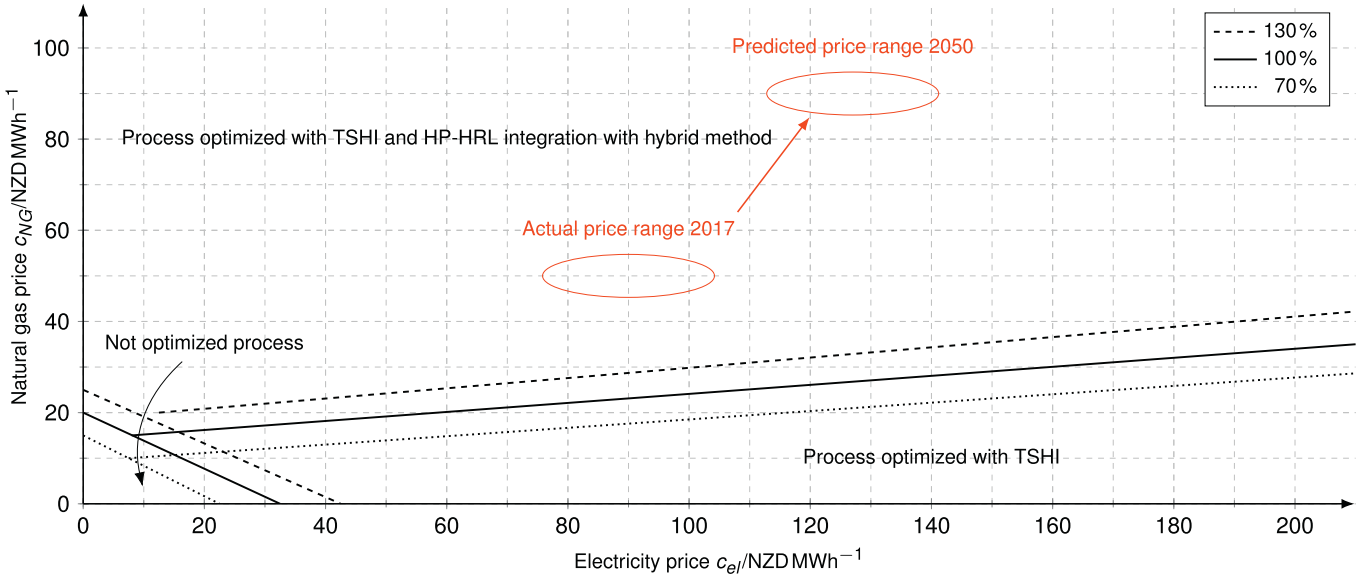

Fig. 11. Sensitivity analysis of TAC concerning natural gas prices and electricity price including an uncertainty of ±30 % for investment costs [40]. Predicted utility costs are estimated from the predicted costs increase of wholesale prices [36].

process integration (e.g. Pinch Analysis) or mathematical programming techniques. In contrast to the expensive mathematical programming methods the hybrid method does not require large computation power which is beneficial in terms of project costs.

The method needs to be developed further, to have an alternative for processes with a large change in the pinch temperature in order to prevent having an extensive temperature lift for the HP. To have a HP that changes its operating condition and characteristics would entail the need for a more detailed model. Still having short computation time for this kind of model is a challenge.

Further work, which is already in progress is addressing the operability of the HP-HRL system. Therefore, a control approach needs to be developed for assuring the demanded condensation and evaporating temperatures.

Acknowledgments

This research project is financially supported by the Swiss Innovation Agency Innosuisse and is part of the Swiss Competence Center for Energy Research SCCER EIP, Switzerland. Further support is provided by the Lucerne University of Applied Sciences and Arts, Switzerland and an international internship at the University of Waikato, New Zealand.

Nomenclature

Latin letters

A	Heat exchanger area (m^2)
C	Costs (NZD)
c	Specific costs (NZD/MWh)
c_p	Specific heat capacity (kJ/kg K)
d_a	Annual operating days (d/y)
F	Lang factor (−)
f_d	Degression factor
h	Film heat transfer coefficient (W/(m^2 K))
I	Cost index (−)
i_r	Interest rate (−)
M	Mass inventory of stroage layer (kg)
$\dot{m}$	Mass flow (kg/s)
m	Transferred mass (kg)
n	Investment period/Plant lifetime (y)
P_{el}	Electrical power (kW)
$\dot{Q}$	Heat flow (kW)
T	Temperature (°C)
T^*	Shifted temperature (°C)
T_P	Pinch temperature (°C)
U	Overall heat transfer coefficient (W/(m^2 K))
V	Storage Volume (m^3)

Greek letters

ΔT	Temperature difference (K)
ΔT_{apr}	Approach temperature (K)
ΔT_{cont}	Contributed temperature difference (K)
ΔT_{lift}	Temperature lift in heat pump (K)
ΔT_{min}	Temperature difference at pinch (K)
Δt_l	Time slice duration (h)
ζ	2nd Law efficiency
η_{drive}	Drive efficiency
ρ	Density (kg/m^3)
ξ	Specific greenhouse gas emissions (t_{CO2e}/MWh)

Subscripts

a	Absorbed, annualized
C	Cold storage
c	Cold storage layer
co	Condensation
$comp$	Compressor
E	Equipment
e	Emitted
el	Electricity
en	Engine
ev	Evaporation
H	Hot storage
h	Hot storage layer
i	Hot process streams ($i \in \{1\ldots,I\}$)
inv	Investment
j	Cold process streams ($j \in \{1\ldots,J\}$)
l	Time slices ($l \in \{1\ldots,L\}$)
m	Hot utilities ($m \in \{1\ldots,M\}$)
n	Cold utilities ($n \in \{1\ldots,N\}$)
op	Operating
S	Supply
s	Process streams ($s \in \{1\ldots,S\}$)
T	Target
tot	Total

Superscripts

$+$	Input to storage
$-$	Output of storage

Abbreviations

AMF	Anhydrous milk fat
CIP	Cleaning-in-place
COP	Coefficient of performance
CT	Cream treatment
CU	Cold utility
GCC	Grand Composite Curve
GHG	Greenhouse gases
HEN	Heat exchanger network
HEX	Heat exchanger
HP	Heat pump
HR	Heat recovery
HRL	Heat recovery loop
HTHW	Hot temperature water
HU	Hot utility
LMTD	Logarithmic mean temperature difference (K)
LTHW	Low temperature hot water
MILP	Mixed integer linear programming
MINLP	Mixed integer nonlinear programming
MPIC	Main plant item costs
NLP	Nonlinear programming
PMEI	Plant, machinery, equipment group index
TAC	Total annual costs
TES	Thermal energy storage
TS	Time slice
TSHI	Total Site Heat Integration

Appendix A. Optimized heat exchanger networks

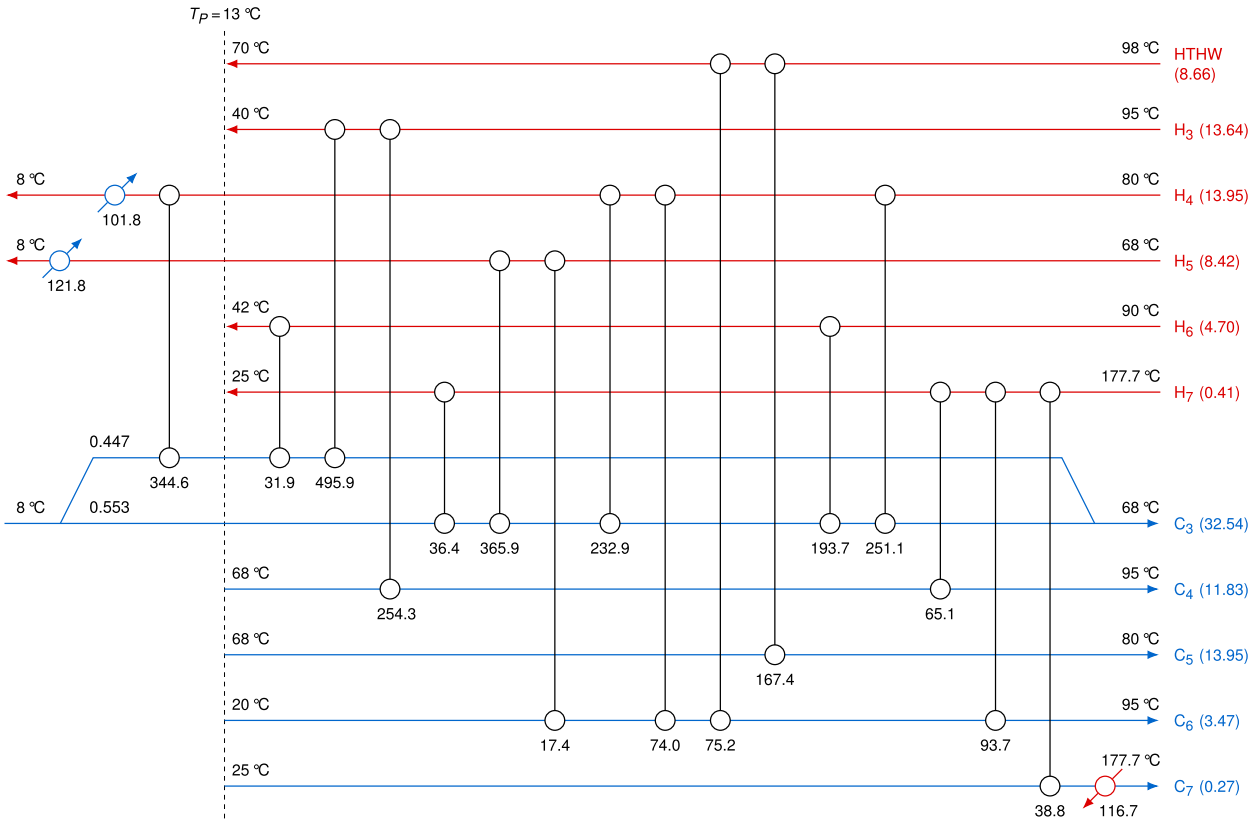

Fig. A.12. Optimized HEN of the AMF production plant without HP-HRL system (*CP* in kW/K values in brackets behind stream number; transferred heat below HEX (kW); fraction of *CP* in branch at split).

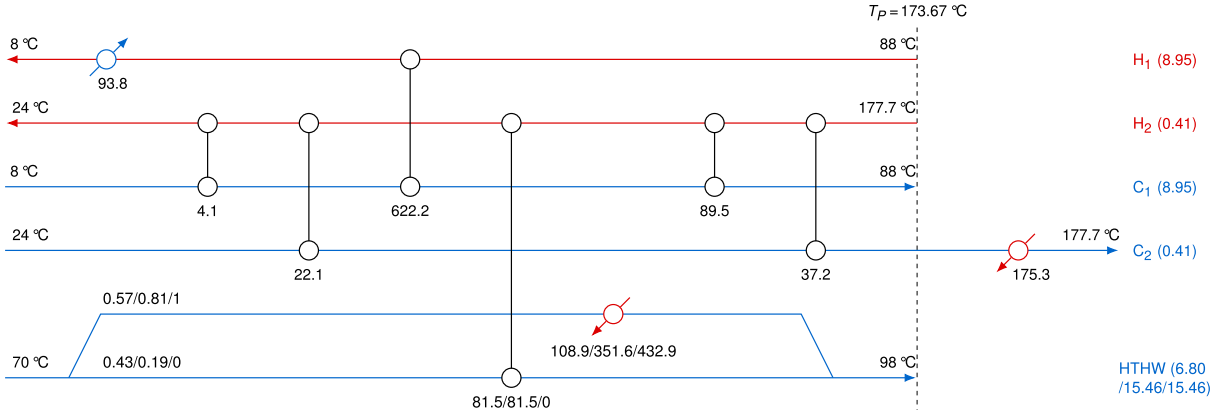

Fig. A.13. Optimized HEN of the CT plant without HP-HRL system (multiple values correspond to different TSs in the following order: $TS_2/TS_3/TS_4$).

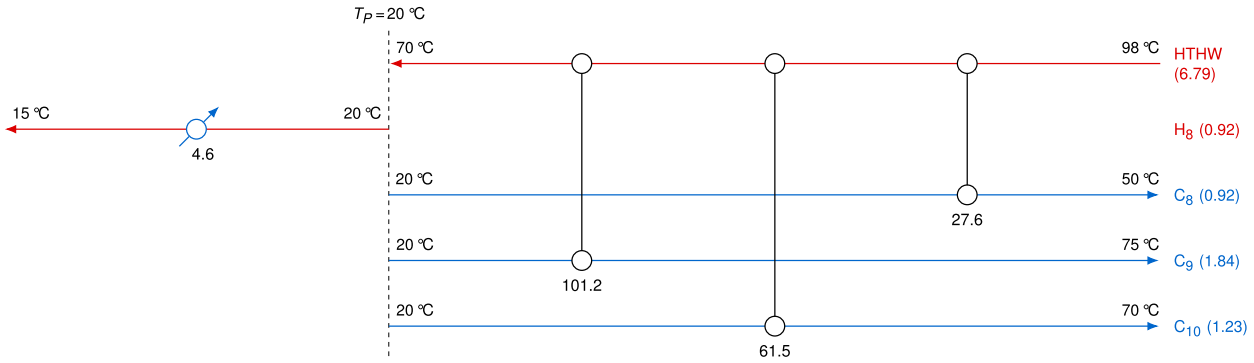

Fig. A.14. Optimized HEN of the CIP system without HP-HRL system.

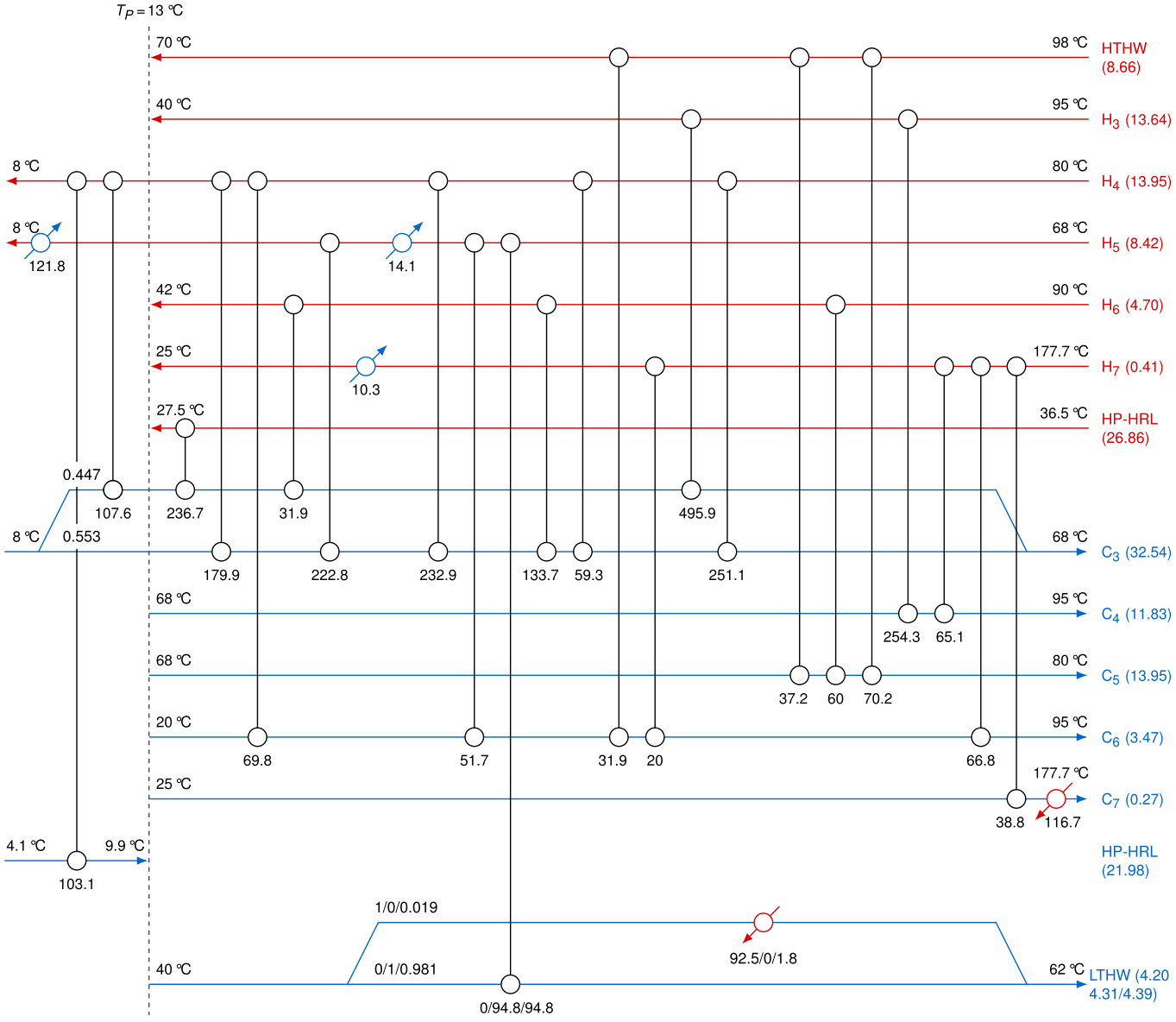

Fig. A.15. Optimized HEN of the AMF production plant with integrated HP-HRL system.

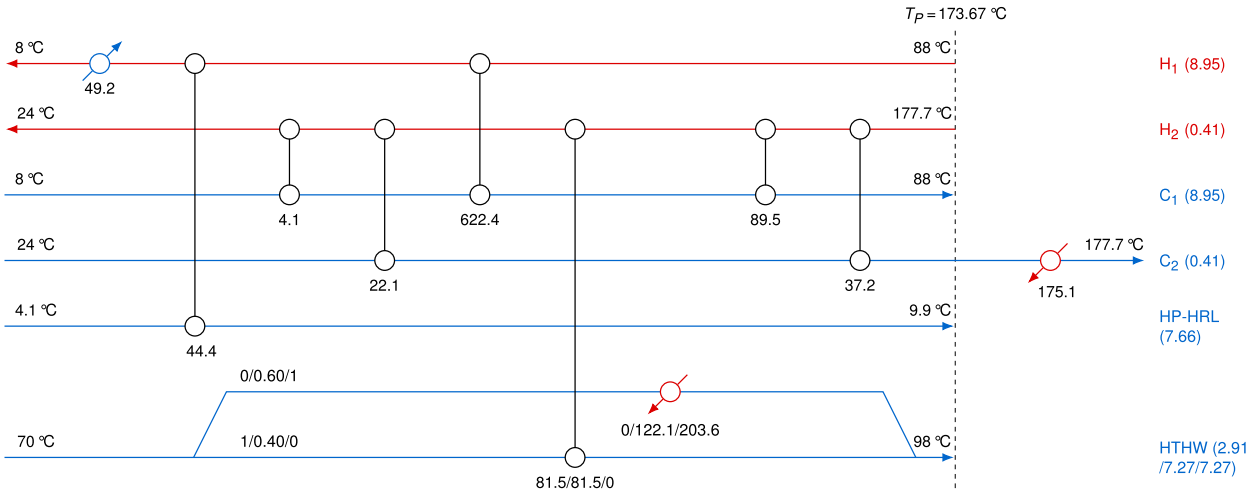

Fig. A.16. Optimized HEN of the CT plant with integrated HP-HRL system.

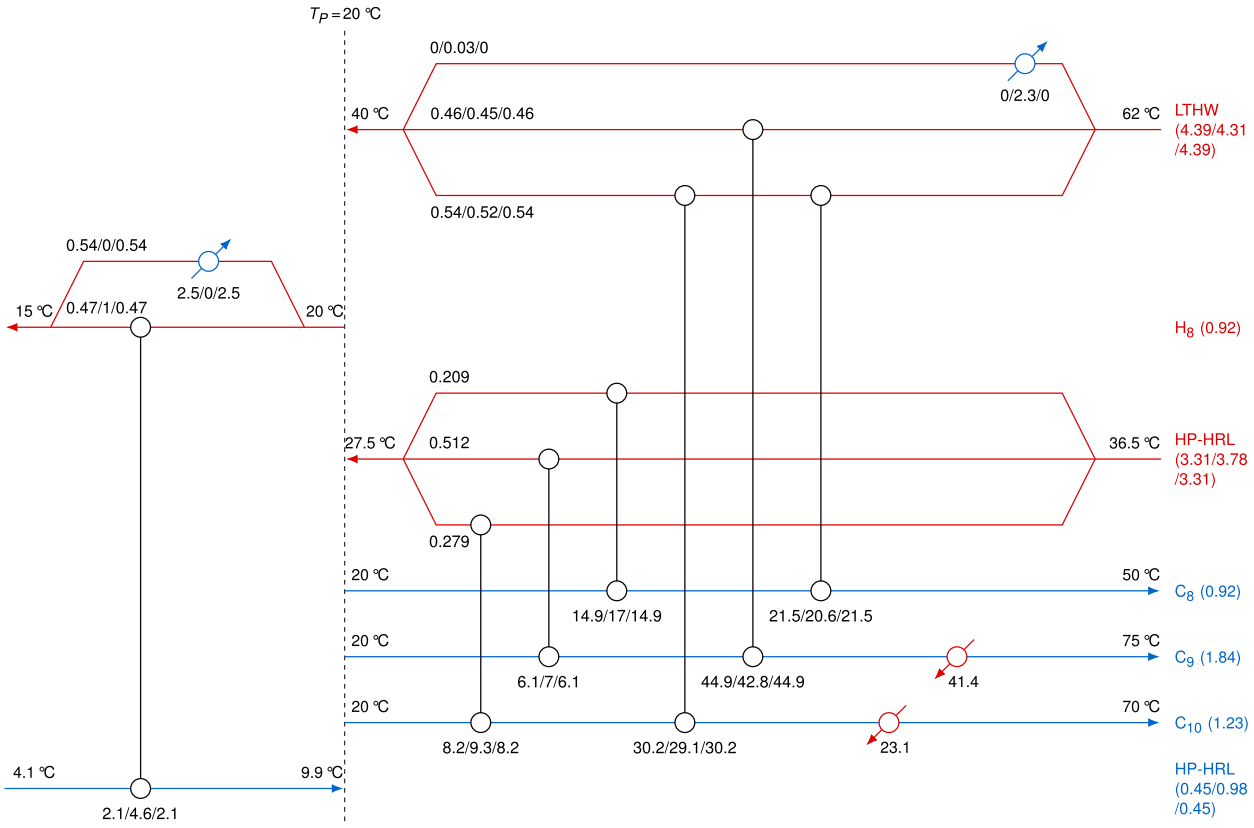

Fig. A.17. Optimized HEN of the CIP system with integrated HP-HRL system.

References

[1] Atkins MJ, Walmsley MR, Morrison AS. Integration of solar thermal for improved energy efficiency in low-temperature-pinch industrial processes. Energy 2010;35(5):1867–73. https://doi.org/10.1016/j.energy.2009.06.039.

[2] Townsend DW, Linnhoff B. Heat and power networks in process design. Part I: criteria for placement of heat engines and heat pumps in process networks. AIChE J 1983;29(5):742–8. https://doi.org/10.1002/aic.690290508.

[3] Ranade SM. New insights on optimal integration of heat pumps in industrial sites. Heat Recovery Syst CHP 1988;8(3):255–63. https://doi.org/10.1016/0890-4332(88)90061-0.

[4] Wallin E, Franck PÅ, Berntsson T. Heat pumps in industrial processes-An optimization methodology. Heat Recovery Syst CHP 1990;10(4):437–46. https://doi.org/10.1016/0890-4332(90)90092-X.

[5] Benstead R, Sharman FW. Heat pumps and pinch technology. Heat Recovery Syst CHP 1990;10(4):387–98. https://doi.org/10.1016/0890-4332(90)90088-2.

[6] Kapustenko PO, Ulyev LM, Boldyryev SA, Garev AO. Integration of a heat pump into the heat supply system of a cheese production plant. Energy 2008;33(6):882–9. https://doi.org/10.1016/j.energy.2008.02.006.

[7] Pavlas M, Stehlík P, Oral J, Klemeš JJ, Kim JK, Firth B. Heat integrated heat pumping for biomass gasification processing. Appl Therm Eng 2010;30(1):30–5. https://doi.org/10.1016/j.applthermaleng.2009.03.013.

[8] Olsen D, Abdelouadoud YL, Liem P, Hoffmann S, Wellig B. Integration of heat pumps in industrial processes. IEA heat pump conference, vol. 12; 2017. p. 1–12.

[9] Shelton MR, Grossmann IE. Optimal synthesis of integrated refrigeration systems-I. Mixed-integer programming model. Comput Chem Eng 1986;10(5):445–59. https://doi.org/10.1016/0098-1354(86)85014-1.
[10] Shelton MR, Grossmann IE. Optimal synthesis of integrated refrigeration systems-II: implicit enumeration scheme. Comput Chem Eng 1986;10(5):461–77. https://doi.org/10.1016/0098-1354(86)85015-3.
[11] Colmenares TR, Seider WD. Heat and power integration of chemical processes. AIChE J 1987;33(6):898–915. https://doi.org/10.1002/aic.690330604.
[12] Holiastos K, Manousiouthakis V. Minimum hot-cold and electric utility cost for a finite-capacity reservoir system. Comput Chem Eng 1999;23(9):1263–76. https://doi.org/10.1016/S0098-1354(99)00288-4.
[13] Holiastos K, Manousiouthakis V. Minimum hot/cold/electric utility cost for heat exchange networks. Comput Chem Eng 2002;26(1):3–16. https://doi.org/10.1016/S0098-1354(01)00726-8.
[14] Oluleye G, Jobson M, Smith R. Process integration of waste heat upgrading technologies. Process Saf Environ Protect 2016;103(Part B):315–33. https://doi.org/10.1016/j.psep.2016.02.003.
[15] Oluleye G, Smith R, Jobson M. Modelling and screening heat pump options for the exploitation of low grade waste heat in process sites. Appl Energy 2016;169:267–86. https://doi.org/10.1016/j.apenergy.2016.02.015.
[16] Oluleye G, Jiang N, Smith R, Jobson M. A novel screening framework for waste heat utilization technologies. Energy 2017;125:367–81. https://doi.org/10.1016/j.energy.2017.02.119.
[17] Wallerand AS, Kermani M, Kantor I, Maréchal F. Optimal heat pump integration in industrial processes. Appl Energy 2018;219:68–92. https://doi.org/10.1016/j.apenergy.2018.02.114.
[18] Maréchal F, Favrat D. Combined exergy and pinch analysis for optimal energy conversion technologies integration. Proceedings of ECOS 2005;18:177–84. 1.
[19] Becker HC, Maréchal F, Vuillermoz A. Process integration and opportunity for heat pumps in industrial processes. In: Proceedings of ECOS, vol. 22; 2009. p. 1381–90.
[20] Becker HC, Spinato G, Maréchal F. A multi-objective optimization method to integrate heat pumps in industrial processes. Computer Aided Chemical Engineering 2011;29:1673–7. https://doi.org/10.1016/B978-0-444-54298-4.50113-6.
[21] Becker HC, Maréchal F. Targeting industrial heat pump integration in multi-period problems. Computer Aided Chemical Engineering 2012;31:415–9. https://doi.org/10.1016/B978-0-444-59507-2.50075-5.
[22] Becker HC, Vuillermoz A, Maréchal F. Heat pump integration in a cheese factory. Appl Therm Eng 2012;43:118–27. https://doi.org/10.1016/j.applthermaleng.2011.11.050.
[23] Chen W, Liang S, Guo Y, Cheng K, Gui X, Tang D. Investigation on the thermal performance and optimization of a heat pump water heater assisted by shower waste water. Energy Build 2013;64:172–81. https://doi.org/10.1016/j.enbuild.2013.04.021.
[24] Miah JH, Griffiths A, McNeill R, Poonaji I, Martin R, Leiser A, et al. Maximising the recovery of low grade heat: an integrated heat integration framework incorporating heat pump intervention for simple and complex factories. Appl Energy 2015;160:172–84. https://doi.org/10.1016/j.apenergy.2015.09.032.
[25] Stampfli JA, Atkins MJ, Olsen DG, Wellig B, Walmsley MRW, Neale JR. Industrial heat pump integration in non-continuous processes using thermal energy storages as utility - a graphical approach. Chemical Engineering Transactions 2018;70:901–6. https://doi.org/10.3303/CET1870151.
[26] Walmsley MRW, Atkins MJ, Walmsley TG. Application of heat recovery loops to semi-continuous processes for process integration. In: Handbook of process integration (PI). Cambridge, UK. Cambridge: Woodhead Publishing; 2013. p. 594–629. https://doi.org/10.1533/9780857097255.4.594. Woodhead Publishing.
[27] Kemp IC, Deakin AW. The cascade analysis for energy and process integration of batch processes. I: calculation of energy targets. Chem Eng Res Des 1989;67(5):495–509.
[28] Wang YP, Smith R. Time pinch analysis. Chem Eng Res Des 1995;73(8):905–14.
[29] Stampfli JA, Atkins MJ, Olsen DG, Wellig B, Walmsley MRW, Neale JR. Industrial heat pump integration in non-continuous processes using thermal energy storages as utility - an NLP enhancement of the graphical approach. Chemical Engineering Transactions 2018;70:1789–94. https://doi.org/10.3303/CET1870299.
[30] Kemp IC. Pinch analysis and process integration - a user guide on process integration for the efficient use of energy. second ed. Oxford, U.K.: Elsevier Ltd; 2007.
[31] Kunz R, Winkelmann B, Mokhatab S. Efficiency and operating characteristics of centrifugal and reciprocating compressors. Pipeline Gas J 2010;237(10).
[32] Linnhoff B, Hindmarsh E. The pinch design method for heat exchanger networks. Chem Eng Sci 1983;38(5):745–63. https://doi.org/10.1016/0009-2509(83)80185-7.
[33] Lang HJ. Simplified approach to preliminary cost estimates. Chem Eng 1948;55(6):112–3.
[34] Stats NZ. Price index by item - plant, machinery and equipment. http://www.stats.govt.nz/infoshare/; 2017.
[35] Chen JJJ. Comments on improvements on a replacement for the logarithmic mean. Chem Eng Sci 1987;42(10):2488–9. https://doi.org/10.1016/0009-2509(87)80128-8.
[36] MBIE. Energy in New Zealand 2017. http://www.mbie.govt.nz/info-services/sectors-industries/energy/energy-data-modelling/publications/energy-in-new-zealand; 2017.
[37] Em6. Electricity market overview. http://www.em6live.co.nz; 2017.
[38] EECA. CO2 emission calculator. https://www.eecabusiness.govt.nz/tools/wood-energy-calculators/co2-emission-calculator/; 2017.
[39] Bylund G. Dairy processing handbook. Tetra Pak Processing Systems; 1995.
[40] Bouman RW, Jesen SB, Wake ML. Process capital cost estimation for New Zealand. Tech. Rep. Society of Chemical Engineers New Zealand; 2004. 2005.
[41] Wächter A, Biegler L. On the implementation of a primal-dual interior-point filter line-search algorithm for large-scale nonlinear programming. Math Program 2006;106:25–57. https://doi.org/10.1007/s10107-004-0559-y.
[42] Philipp M, Schumm G, Peesel RH, Walmsley TG, Atkins MJ, Schlosser F, et al. Optimal energy supply structures for industrial food processing sites in different countries considering energy transitions. Energy 2018;146:112–23. https://doi.org/10.1016/j.energy.2017.05.062.